The Endocannabinoid Anandamide Protects Neurons during CNS Inflammation by Induction of MKP-1 in Microglial Cells

Eva Eljaschewitsch,[1] Anke Witting,[8] Christian Mawrin,[3] Thomas Lee,[5] Peter M. Schmidt,[1] Susanne Wolf,[6] Heide Hoertnagl,[5] Cedric S. Raine,[7] Regine Schneider-Stock,[2] Robert Nitsch,[4,9] and Oliver Ullrich[1,9,*]

[1] Institute of Immunology
[2] Institute of Pathology and
[3] Institute of Neuropathology
Medical Faculty
Otto-von-Guericke-University Magdeburg
Leipziger Str. 44
39120 Magdeburg
Germany
[4] Center for Anatomy and
[5] Institute of Pharmacology
Charité University Hospital Berlin
Schumannstr. 20/21
10098 Berlin
Germany
[6] Max-Delbrueck-Center of Molecular Medicine
Berlin-Buch
Robert-Rössle-Str. 10
13092 Berlin
Germany
[7] Albert Einstein College of Medicine
1300 Morris Park Avenue
New York, New York 10461
[8] Magnuson Health Science Center
University of Washington
1914 Pacific Street NE
Seattle, Washington 98195

Summary

Endocannabinoids are released after brain injury and believed to attenuate neuronal damage by binding to CB_1 receptors and protecting against excitotoxicity. Such excitotoxic brain lesions initially result in primary destruction of brain parenchyma, which attracts macrophages and microglia. These inflammatory cells release toxic cytokines and free radicals, resulting in secondary neuronal damage. In this study, we show that the endocannabinoid system is highly activated during CNS inflammation and that the endocannabinoid anandamide (AEA) protects neurons from inflammatory damage by $CB_{1/2}$ receptor-mediated rapid induction of mitogen-activated protein kinase phosphatase-1 (MKP-1) in microglial cells associated with histone H3 phoshorylation of the *mkp-1* gene sequence. As a result, AEA-induced rapid MKP-1 expression switches off MAPK signal transduction in microglial cells activated by stimulation of pattern recognition receptors. The release of AEA in injured CNS tissue might therefore represent a new mechanism of neuro-immune communication during CNS injury, which controls and limits immune response after primary CNS damage.

*Correspondence: oliver.ullrich@medizin.uni-magdeburg.de
[9] These authors contributed equally to this work.

Introduction

The endocannabinoid system, consisting of cannabinoid receptors, their endogenous ligands, and enzymes for synthesis and degradation of endocannabinoids, is known to play a crucial role in neuronal signal transduction. Cannabinoid-sensitive sites inside the brain include the neuronal CB_1 cannabinoid receptor (Matsuda et al., 1988) and its counterpart in the immune system, the CB_2 receptor (Munro et al., 1993). The endogenous ligands, the endocannabinoids, are made through cleavage of membrane precursors and are involved in various signaling processes. Whereas the metabolic pathways of anandamide (AEA), a small lipid molecule sharing structural features with the eicosanoids, are unique and release of the compound in the living brain occurs on demand (Di Marzo et al., 1994; Giuffrida et al., 1999; Walker et al., 1999), 2-arachidonoylglycerol (2-AG) has been detected in much higher concentrations in brain tissue than anandamide, is formed in central intersections of lipid metabolism, and is therefore suggested to be engaged in housekeeping functions, additionally to its signaling functions (Sugiura et al., 1995; Mechoulam et al., 1995; Piomelli and Greengard, 1990, Piomelli, 2003). During neuronal activity, the endogenous cannabinoid AEA is formed by glutamate receptor agonists in a Ca^{2+}-dependent manner or by stimulation of dopamine D_2 receptors in a G-protein-coupled process (Giuffrida et al., 1999). In the neuronal network, endocannabinoids mediate a localized signaling mechanism through which principal neurons modify the strength of incoming synaptic inputs (Alger, 2002; Wilson and Nicoll, 2002): in the CA1 field of the hippocampus, membrane depolarization opens voltage-activated Ca^{2+} channels in pyramidal neurons and therefore stimulates the synthesis of 2-AG and AEA. The endocannabinoids then travel backward across the synapse to interact with CB_1 receptors on axon terminals of GABAergic interneurons, leading to depolarization-induced suppression of inhibition (DSI). Such retrograde signaling by endocannabinoid-mediated DSI occurs in the hippocampus but has also been shown outside the hippocampus at interneuron-principal cell synapses (Llano et al., 1991; Kreitzer and Regehr, 2001; Trettel and Levine, 2003).

Interestingly, endogenous cannabinoids are also released after brain injury (Panikashvili et al., 2001; Hansen et al., 2001; Marsicano et al., 2003; Mechoulam and Lichtman, 2003; Franklin et al., 2003) and are believed to attenuate neuronal damage by binding to CB_1 receptors (Panikashvili et al., 2001; Hansen et al., 2001; Marsicano et al., 2003) and protecting against excitotoxicity (Marsicano et al., 2003; Mechoulam and Lichtman, 2003). Such excitotoxic brain lesions initially result in primary destruction of brain parenchyma, which attracts macrophages and microglia, the major effector cells within the CNS. These inflammatory cells produce large amounts of toxic cytokines and oxygen radicals that subsequently result in secondary neuronal damage. Although it is known that the cannabinoid receptors CB_1 and CB_2 are expressed on microglial cells (Carrier et al., 2004;

Facchinetti et al., 2003; Waksman et al., 1999) and that activated microglia are capable of producing larger amounts of endogenous cannabinoids than neurons (Walter et al., 2003), the function of the endocannabinoid system within the CNS immune system has not been elucidated. In this study, we reveal a function of the endocannabinoid system not related to neurons but affecting nerve cell function and survival after brain injury. We show that the endocannabinoid system is highly activated during CNS inflammation and protects neurons from inflammatory damage by inducing a novel intracellular negative feedback loop in microglial cells acting via $CB_{1/2}$-mediated epigenetic regulation of MKP-1 expression.

Results

The Endocannabinoid System Is Activated during CNS Inflammation and Protects Neurons from Inflammatory Damage

To investigate whether the endocannabinoid system is activated during inflammation within the brain parenchyma, we first analyzed endocannabinoid concentrations in CNS tissue from inflammatory lesions of patients with active or silent multiple sclerosis (MS) and normal control patients by gas chromatography/mass spectrometry (GC/MS) (Witting et al., 2004a). In inflammatory lesions of patients with active MS, we found a 3.7-fold higher concentration of the endocannabinoid anandamide (AEA) and a 1.9-fold higher concentration in lesions of patients with silent MS, in comparison to healthy controls (Figure 1A). Levels of other endocannabinoids, such as 2-arachidonoylglycerol (2-AG) and palmitoylethanolamide (PEA), were only slightly influenced (data not shown). Because damage to neuronal structures has only recently been suggested to be a key mechanism during the development of MS (Trapp et al., 1998; Hemmer et al., 2002), we next addressed the question of whether the accumulation of AEA might be a direct consequence of neuronal damage or because of invading immune cells. Thus, we used an approach that allows the study of the effects of immunoeffector cell invasion into living organotypic brain tissue, the organotypic hippocampal slice culture system (OHSC) (Heppner et al., 1998; Ullrich et al., 2001; Diestel et al., 2003). In this model, exogenously cultivated microglia migrate into OSHCs toward the site of neuronal injury (Heppner et al., 1998), where they induce inflammatory conditions and associated tissue reactions (Heppner et al., 1998; Ullrich et al., 2001; Diestel et al., 2003). In living brain tissue, we detected a 2.8-fold increase in AEA concentration after induction of specific excitotoxic neuronal damage by N-methyl-D-aspartate (NMDA) that was potentiated up to a 13.2-fold increase after invasion of BV-2 microglial cells (Figure 1B). BV-2 microglial cells exhibit morphologic and functional features comparable to primary microglial cells (Diestel et al., 2003; Bocchini et al., 1992) and did not induce AEA production in a resting state (Figure 1B).

Because AEA accumulated in inflamed brain tissue, the question arises about its influence on inflammatory damage to neurons. To address this, we transferred BV-2 microglial cells onto excitotoxically damaged OHSCs from mice and quantified the damage in the neuronal cell layers (pyramidal cell layer of the cornu ammonis and granule cell layer of the dentate gyrus) after 3 days (Ullrich et al., 2001; Adamchik et al., 2000; Laake et al., 1999). As demonstrated in Figure 1C, incubation with NMDA resulted in primary neuronal damage that was potentiated by the invasion of microglial cells, resulting in severe secondary damage. Incubation with 2 μM AEA completely abolished inflammatory damage but not the primary excitotoxic damage (Figure 1C). Incubation with AEA alone did not increase neuronal damage (Figure 1C). In order to investigate whether this AEA-mediated protection occurred as a consequence of other mechanisms of neuronal cell damage, we subjected OHSCs to oxygen glucose deprivation (OGD) and assessed neuronal survival after 3 days of microglial invasion, as described above. Here, incubation with 2 μM AEA reduced neuronal damage to the level of OGD-induced primary damage (Figure 1D). Because we observed no direct protection of neurons by AEA, neither in the NMDA nor in the OGD model in OHSCs, we investigated the protection of primary neurons subjected to NMDA- or OGD-induced injury in isolated primary neurons by measurement of LDH activity (Figure 1E): 2 μM AEA was not capable of protecting primary neurons directly against NMDA, which was also the case after OGD (319.2 ± 36.5 U/ml LDH release 24 hr after OGD versus 359.2 ± 22.3 U/ml LDH release 24 hr after OGD + AEA). These data indicate that the endocannabinoid AEA protects neurons from inflammatory damage very efficiently, but not from direct injury resulting from excitotoxicity or oxygen-glucose deprivation.

In order to investigate a possible protective role of the endogenous cannabinoid system during the development of inflammatory neuronal damage, we transferred BV-2 microglial cells onto the surface of NMDA-damaged OHSCs in the presence of 0.5 μM AM 251, a specific CB_1 receptor antagonist, and 2 μM AM 630, a specific CB_2 receptor antagonist, and assessed damage in the neuronal layers of the hippocampus after 3 days. In this experiment, cannabinoids were not added to the brain tissue, and only the activity of endogenously formed cannabinoids was addressed. To allow the detection of a possible further enhancement of inflammatory neuronal damage after cannabinoid receptor inhibition, we reduced the time of primary NMDA-damage (2 hr instead of 4 hr compared to Figure 1C), resulting in lower primary and secondary inflammatory neuronal damage (2.4-fold and 4.1-fold, respectively, Figure 2) as baseline. CB_2 receptor inhibition elevated the extent of inflammatory damage by 40% (from 4.1-fold to 5.8-fold), whereas CB_1 receptor inhibition had no effect (Figure 2). In conclusion, the endocannabinoid system protects neurons from inflammatory damage in a CB_2 receptor-dependent manner.

Activity on Cannabinoid Receptors Suppresses Inflammatory Attack in Healthy Brain Tissue

Interestingly, without primary neuronal damage, BV-2 microglial cells release only small amounts of nitric oxide (2.28 ± 0.14 μM without neuronal damage versus 15.62 ± 2.66 μM after neuronal damage) and affect neuronal viability only slightly (Figure 2). This means that microglial cells, although present in large amounts inside the living OHSC tissue, are obviously under strict control in a healthy brain enviroment. In contrast, after

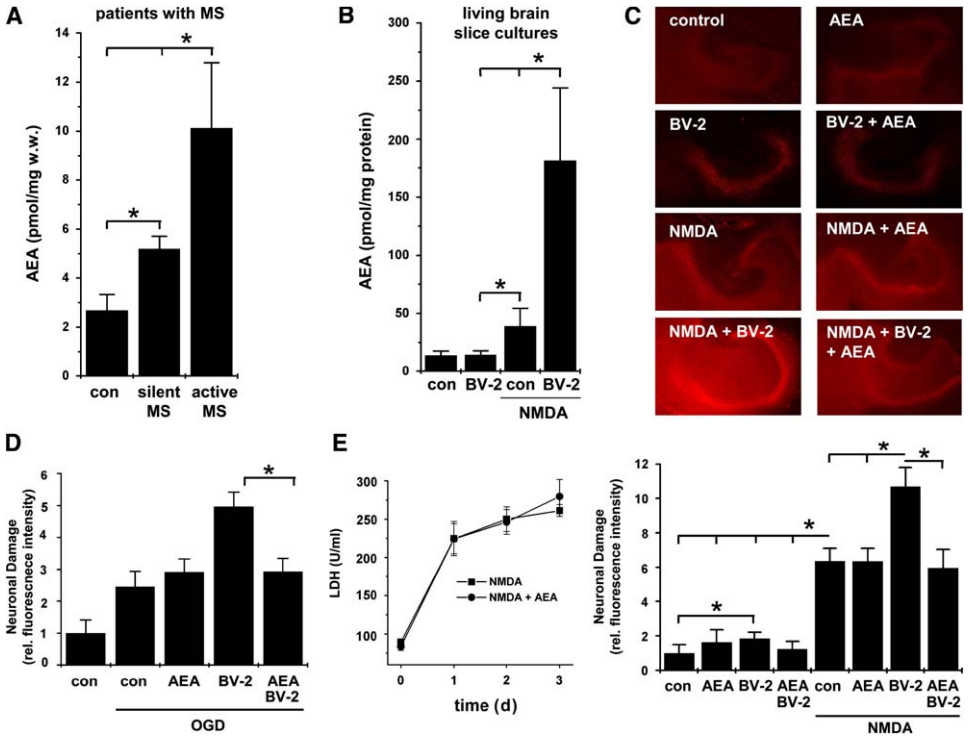

Figure 1. The Endocannabinoid System Is Activated during CNS Inflammation and Protects Neurons from Inflammatory Damage

(A) Accumulation of AEA in inflammatory lesions of patients with multiple sclerosis. Absolute anandamide (AEA) concentrations detected by GC/MS[10] are demonstrated for control patients and patients with chronic silent or active MS lesions. Data are given as mean ± S.D. con, control patients (n = 7); silent MS (n = 6); and active MS (n = 5); asterisk, $p < 0.05$ (active MS versus silent MS and controls, silent MS versus controls).

(B) Accumulation of AEA in living brain tissue after invasion of microglial cells. Concentration of anadamide (AEA) in the living brain tissue of hippocampal slice cultures (OHSCs) after initial specific neuronal damage induced by 5 μM NMDA with or without transfer of 10^5 BV-2 microglial cells (BV-2), in comparison to untreated controls (con). Data are given as mean ± S.D., n = 3 for each group. Asterisk, $p < 0.05$ (BV-2 after NMDA damage versus NMDA damage without BV-2 and BV-2 without NMDA damage, NMDA damage versus BV-2 without NMDA damage).

(C) Top: pictures of propidium iodide fluorescence microscopy of the regions of neuronal injury in the cornu ammonis and dentate gyrus in living organotypic brain slice cultures after NMDA damage. Con, no treatment; AEA, incubation with 2 μM AEA; NMDA, induction of primary neuronal damage with 5 μM NMDA for 4 hr; BV-2, 3 days after transfer of 10^5 BV-2 microglial cells. One representative picture of each group is shown.

(C) Bottom: propidium iodide fluorescence in the neuronal cell layers after NMDA damage. Results are given as propidium iodide fluorescence in the neuronal layers after treatment relative to nondamaged brain tissue. Control, no treatment; AEA, incubation with 2 μM AEA; NMDA, induction of primary neuronal damage with 5 μM NMDA for 4 hr; BV-2, 3 days after transfer of 10^5 BV-2 microglial cells. Data are given as mean ± S.D. (n = 6); asterisk, $p < 0.05$ (BV-2 + AEA versus BV-2 and BV-2 versus AEA or con in the NMDA treated group, NMDA damage versus AEA, BV-2 + AEA, BV-2 and con in the nondamaged group, BV-2 versus con in the nondamaged group).

(D) Propidium iodide fluorescence in the neuronal cell layers after oxygen glucose deprivation. Results are given as propidium iodide fluorescence in the neuronal layers after treatment relative to nondamaged brain tissue. con, no treatment; AEA, incubation with 2 μM AEA; OGD, oxygen glucose deprivation, BV-2, 3 days after transfer of 10^5 BV-2 microglial cells. Data are given as mean ± S.D. (n = 6); asterisk, $p < 0.05$ (BV-2 + AEA versus BV-2).

(E) No direct protection of neurons by AEA from excitotoxic damage. Release of LDH activity after incubation with 5 μM NMDA with or without 2 μM AEA is demonstrated. Data are given as mean ± S.D. (n = 3).

cannabinoid receptor inhibition, neuronal damage exacerbates to 3.6-fold after CB_1 receptor inhibition and to 3.8-fold after CB_2 receptor inhibition (Figure 2). Thus, activity on CB_1 and CB_2 cannabinoid receptors suppresses microglial cell attack on healthy brain tissue and therefore prevents the CNS from endogenous inflammatory damage as a potential nondesired side effect of continuous immune surveillance. Conversely, downregulation of the endocannabinoid system might therefore result in a loss of control and an ongoing attack of microglial cells on neurons.

$CB_{1/2}$-Dependent ERK-1/2 Dephosphorylation and Suppression of Nitric Oxide Synthesis in Activated Microglial Cells

In the next set of experiments, we examined the pathway that prevents invading immunoeffector cells from initiating severe inflammatory damage. For this, we investigated the release of proinflammatory cytokines in cultured BV-2 microglial cells and of the cytotoxic free radical nitric oxide (NO) after stimulation with lipopolysaccharide (LPS), which acts via CD14/TLR4. In these experiments, we revealed a distinct dose-dependent reduction of NO release by AEA (Figure 3A, left), and also by the $CB_{1/2}$ agonist WIN 55,212-2 (Figure 3A, right), associated with suppression of inducible nitric oxide synthetase (iNOS) (Figure 3C). Moreover, release of the proinflammatory cytokine IL-6 was delayed (381 ± 47 pg/ml with 2 μM AEA versus 1095 ± 254 pg/ml without AEA after 12 hr) but reached similar levels after 24 hr. In contrast, release of TNF-α was not impaired (data not shown). Excessive production of NO has been postulated to elicit immune-mediated neurodegenerative inflammatory processes and to cause brain injury

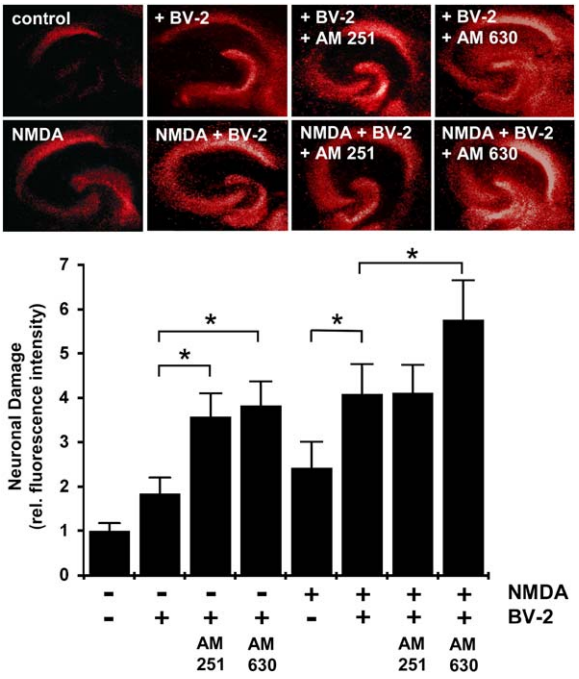

Figure 2. Endogenous Cannabinoid Receptor Activation Protects Neurons in Damaged and Healthy Brain Tissue

Top: pictures of propidium iodide fluorescence microscopy of the regions of neuronal injury in the cornu ammonis and dentate gyrus in healthy living organotypic brain slice cultures or after NMDA damage. Control, no treatment; NMDA, induction of primary neuronal damage with 5 μM NMDA for 2 hr; BV-2, 3 days after transfer of 10^5 BV-2 microglial cells; AM 251, incubation with 0.5 μM of the CB_1 receptor antagonist AM 251; AM 630, incubation with 2 μM of the CB_2 receptor antagonist AM 630. One representative picture of each group is shown. Bottom: propidium iodide fluorescence in the neuronal cell layers in healthy OHSC tissue or after NMDA damage. Results are given as propidium iodide fluorescence in the neuronal layers after treatment relative to nondamaged brain tissue, legend as in top panel. Data are given as mean ± S.D. (n = 6); asterisk, $p < 0.05$ (BV-2 + AM 630 versus BV-2 and with BV-2 versus without BV-2 in the NMDA damaged group, BV-2 + AM 630 versus BV-2 and BV-2 + AM 251 versus BV-2 in the nondamaged group) with 0.5 μM of the CB_1 receptor antagonist AM 251; AM 630, incubation with 2 μM of the CB_2 receptor antagonist AM 630. One representative picture of each group is shown.

(Mabuchi et al., 2000; Stoll et al., 1998). To clarify whether the abrogated NO release was due to specific interaction between AEA and $CB_{1/2}$ receptors, we incubated OHSCs infiltrated with microglia with the pharmacological antagonists AM251 to CB_1 and AM630 to CB_2 receptors. In these experiments, we showed that the abolished NO release at least partially returns after incubation with both antagonists and that CB_2 blockade was more effective than CB_1 blockade (Figure 3B). This was also supported by experiments with blocking antibodies against CB_1 and CB_2 receptors, which restored the NO release to 21.2 ± 0.9 μg/ml (anti-CB_1) or 7.21 ± 0.34 μg/ml (anti-CB_2), respectively. Therefore, we conclude that AEA is capable of suppressing NO release in microglial cells inside inflamed brain tissue via interactions with $CB_{1/2}$ receptors.

Next, we addressed the question of which signaling pathway might be responsible for suppressed microglia activation by LPS/AEA coincubation. Incubation with AEA alone caused Thr202/Thr204 phosphorylation of extracellular signal-regulated kinase-1/2 (ERK-1/2) after 8 hr (Figure 4A) as a consequence of activation of the mitogen-activated protein kinase (MAPK) pathway, as reported previously (Derkinderen et al., 2003). LPS alone induced ERK-1/2 phosphorylation after 2 hr (Figure 4A). Surprisingly, in the presence of both stimuli (1 hr preincubation with AEA or WIN 55,212-2 followed by LPS stimulation), phosphorylation of ERK-1/2 was not potentiated or even sustained but was reduced (Figure 4B). In this case, as a result of 1 hr preincubation with AEA (Derkinderen et al., 2003), the initial ERK-1/2 phosphorylation disappeared completely after LPS stimulation. Therefore, we assume that anandamide sets microglial cells into a state of alert by rapid MAPK-phosphorylation, but prevents (over-)activation in the presence of a second stimulus. The phosphorylation state of ERK-1/2 is generally regulated by the balance of upstream kinases or phosphatases. But in contrast to the rapid phosphorylation of ERK kinase (MEK) in microglial cells after LPS treatment alone (Figure 4C), LPS treatment after preincubation and in the presence of AEA or WIN 55,212-2 reduced and delayed MEK phosphorylation (Figure 4C). Because the constant or enhanced MEK activation after LPS treatment in the presence of AEA or WIN 55,212-2 (Figure 4C) did not account for ERK-1/2 dephosphorylation (Figure 4B), we next focused on the regulation of ERK-1/2-dephosphorylating phosphatases by AEA.

Anadamide Induced MKP-1, which Colocalized with Invading Microglial Cells in Inflammatory Lesions of Patients with Multiple Sclerosis

In these experiments, a rapid induction of mitogen-activated protein kinase-phosphatases-1 and -2 (MKP-1 and MKP-2) occurred within 1 hr of treatment WIN 55,212-2 and within 2 hr of treatment with AEA combined with LPS (Figure 5B): induction of MKP-1 and MKP-2 protein expression occurred early after the onset of cannabinoid receptor stimulation. Here, we observed maximal induction of MKP-1 and MKP-2 after 2 hr AEA treatment, whereas LPS resulted in MKP-1 induction after 12 hr and MKP-2 induction after 4 hr (Figure 5A). This time course indicated that MKP-1 and MKP-2 induction was a direct effect of $CB_{1/2}$ stimulation rather than an indirect effect triggered by initial MAPK activation (Shapiro and Ahn, 1998). Moreover, incubation with Ro-318220, an inhibitior of MKP expression (Guo et al., 1998), prevented ERK-1/2 dephosphorylation in cultured microglial cells costimulated with AEA/LPS (Figure 5C). These findings suggest a pivotal role of MKP-1 and MKP-2 in the regulation and control of inflammatory reactions within the CNS. Thus, we investigated whether invading microglial cells in inflammatory lesions in the CNS actually expressed MKP-1 and MKP-2 and analyzed brain tissue from patients with MS by double-fluorescence microscopy (Figure 6A). As shown in representative pictures in Figure 6A, we found expression of MKP-1 in cells of inflammatory brain lesions colocalized with Ox42-positive microglia in the presence of high AEA concentrations (Figure 1A) but much lower expression and lack of colocalization of MKP-2 with microglial cells. Thus, we conclude that MKP-1 is indeed expressed in microglia cells during CNS inflammation (Figure 6A) induced by high levels of the endocannabinoid

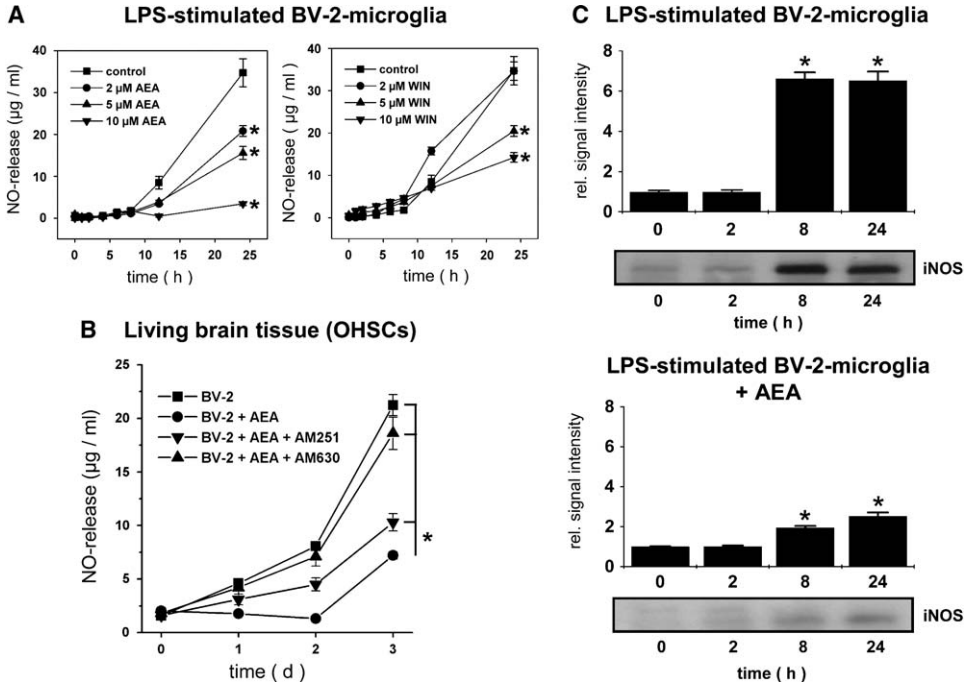

Figure 3. $CB_{1/2}$-Dependent Suppression of Nitric Oxide Synthesis and Nitric Oxide Synthetase Induction in Activated Microglial Cells

(A) $CB_{1/2}$ stimulation by AEA or WIN 55,212-2 abrogates nitric oxide release. BV-2 microglial cells were incubated with 2, 5, 10 µM AEA (left) or 2, 5, 10 µM WIN 55,212-2 for 1 hr before activation by LPS. Data are given as mean ± S.D. (n = 6); asterisk, $p < 0.05$ at 24 hr (2, 5, or 10 µM AEA or 2, 5, 10 µM WIN versus con without treatment).

(B) Reduction of NO release in microglia-invaded living brain tissue by AEA is $CB_{1/2}$ dependent. NMDA-damaged organotypic hippocampal brain slice cultures were incubated with 2 µM AEA after transfer of 10^5 BV-2 microglial cells in the presence of 0.5 µM of the CB_1 receptor antagonist AM 251 or 2 µM of the CB_2 receptor antagonist AM 630. Data are given as mean ± S.D. (n = 3). Asterisk, $p < 0.05$ at 24 hr (BV-2 + AEA versus BV-2 + AEA + AM 251 or BV-2 + AEA+ AM 630 or BV-2 without treatment).

(C) Reduction of iNOS expression by AEA in activated microglia. BV-2 microglial cells were activated by LPS with (bottom) or without (top) co-incubation with 2 µM AEA. Data are given as signal intensity relative to 0 min (mean ± S.D., n = 3). Asterisk, $p < 0.05$ (time points versus 0 min). One representative immunoblot is demonstrated.

AEA (Figure 1A). Because formation of inflammatory lesions (Figure 6A) depends strongly on cell migration and because cannabinoid-receptor stimulation increase microglia cell migration in vitro (Walter et al., 2003), we next tested whether CB_1- or CB_2-receptor activity is required for migration of microglial cells into the regions of neuronal injury in living brain slice cultures. We found that site-specific microglia migration is strongly disturbed in the presence of the CB_1- and CB_2-receptor antagonists AM251 and AM630, respectively (Figure 6B).

Differential Regulation of MAPK Signal Transduction by AEA Depends on the Presence of a Second Signal

Signals of LPS or AEA alone are transduced via the MAPK pathway and resulted in an elevated and sustained ERK-1/2 phosphorylation (Figure 4C). Moreover, LPS stimulation induced ERK-1/2 phosphorylation more rapidly (after 2 hr) than AEA stimulation (after 8 hr). Sustained ERK-1/2 phosphorylation was associated with slowly increasing MKP-1 induction after 12 hr (Figure 5A), which might represent a negative feedback loop of MAPK activation as described earlier (Shapiro and Ahn, 1998). But in contrast, in the presence of both LPS and AEA, MKP-1 was induced rapidly and significantly after 2 hr, reached expression levels higher than after LPS or AEA stimulation alone, and remained constantly elevated (Figure 5B). As a consequence, stimulation with LPS was not capable of inducing ERK-1/2 phosphorylation in the presence of AEA but became almost completely dephosphorylated after 24 hr (Figure 4B). Initial ERK-1/2 phosphorylation as shown in Figure 4B results from 1 hr preincubation with AEA alone before stimulation with LPS.

In order to verify our assumption that MKP-1 induction is not a secondary consequence of MAPK pathway activation (Shapiro and Ahn, 1998), we incubated LPS-stimulated microglial cells with the MEK inhibitor U0126 and found no difference in MKP-1 expression after 12 hr treatment in the presence of AEA but a complete abrogation of MKP-1 expression after treatment with LPS alone (Figure 7A). Moreover, in the presence of CB_1 or CB_2 antagonists, AEA failed to induce MKP-1 expression (Figure 7B). Therefore, we conclude that AEA-induced MKP-1 expression is a primary, $CB_{1/2}$-mediated effect and not secondary to MAPK activation. To investigate whether the neuroprotective effect of AEA is mediated by MAPK activation or by $CB_{1/2}$ stimulation or both, we then assessed cell damage in the neuronal layers of OHSCs invaded by microglial cells as described above (Figure 7C). In these experiments, we found that MAPK-pathway inhibition by U0126 did not influence neuroprotection, whereas it was attenuated by CB_1 inhibition and completely abrogated by CB_2 inhibition (Figure 7C). Taken together, AEA alone activates

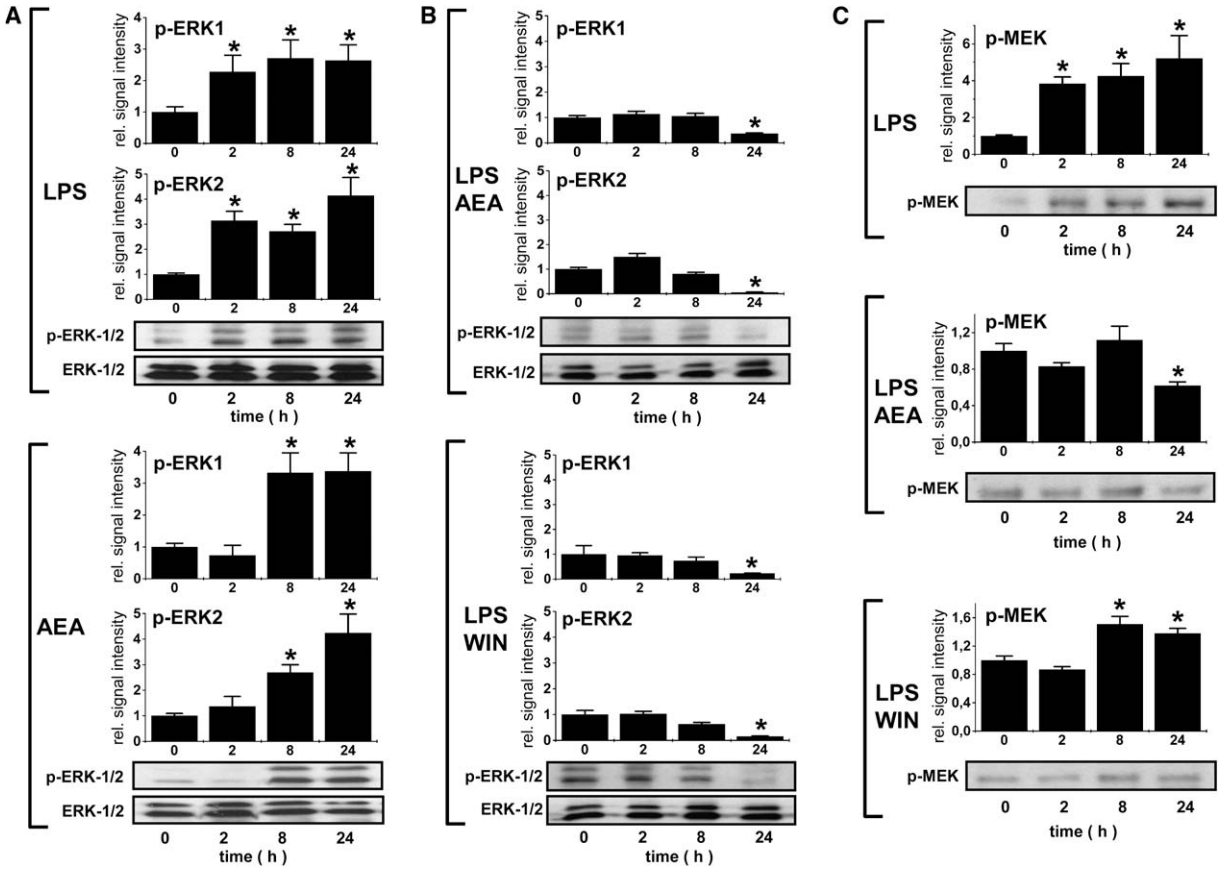

Figure 4. $CB_{1/2}$-Dependent ERK-1/2 Phosphorylation in Resting Microglial Cells and ERK-1/2 Dephosphorylation in Activated Microglial Cells

(A) ERK-1/2 phosphorylation in stimulated microglial cells in the presence of AEA. ERK-1/2 is phosphorylated after incubation with AEA or LPS. BV-2 microglial cells were incubated with 10 μg/ml LPS (top) or with 2 μM AEA (bottom). Data are given as signal intensity of p-ERK-1 and p-ERK-2 relative to 0 min (mean ± S.D., n = 3). Asterisk, $p < 0.05$ (time points versus 0 min). One representative immunoblot is demonstrated.

(B) ERK-1/2 dephosphorylation in LPS-activated microglial cells in the presence of AEA or WIN-55,212,-2. ERK-1/2 is dephosphorylated in LPS-activated BV-2 microglial cells after incubation with 2 μM AEA (top) or 2 μM WIN 55,212-2, a $CB_{1/2}$-receptor agonist (bottom). Data are given as signal intensity of p-ERK-1 and p-ERK-2 relative to 0 min (mean ± S.D., n = 3). Asterisk, $p < 0.05$ (time points versus 0 min). One representative immunoblot is demonstrated.

(C) Reduction of MEK-phosphorylation in LPS-activated microglial cells in the presence of AEA or WIN-55,212-2. MEK phosphorylation is reduced in LPS-activated BV-2 microglial cells after incubation with 2μM AEA (top) or 2 μM WIN 55,212-2, a $CB_{1/2}$-receptor agonist (bottom). Data are given as signal intensity of p-MEK relative to 0 min (mean ± S.D., n = 3). Asterisk, $p < 0.05$ (time points versus 0 min). One representative immunoblot is demonstrated.

MAPK pathway, but switches off MAPK signal transduction by rapid MKP-1 induction in the presence of a second stimuli on microglial pattern recognition receptors.

Anandamide Induced Rapid Phosphorylation of Histone H3 on the mkp-1 Gene and MKP-1 Expression in Microglial Cells, which Suppresses Nitric Oxide Release and Inflammatory Damage in Living Brain Tissue

To investigate whether blocking of NO release by AEA was the result of MKP-1 induction, we transferred BV-2 microglial cells—either transfected with MKP-1 siRNA or control siRNA to OHSCs—and followed the release of NO during the inflammatory process over the course of 3 days (Figure 7D). Here, microglial cells with silenced MKP-1 responded very weakly to AEA incubation compared to the controls, suggesting that the reduced NO release in the presence of AEA (Figure 3A) was indeed MKP-1 dependent (Figure 5B). As a consequence of the functional role of microglial MKP-1 during endocannabinoid-mediated cell-to-cell communication during CNS inflammation, we focused on the regulation of *mkp-1* gene expression. Whereas little is known about the transcriptional regulation of *mkp-1*, direct and fast regulation of *mkp-1* by phosphorylation of histone H3 has been previously reported (Li et al., 2001). Thus, we performed chromatin-immunoprecipitation experiments with an anti-phospho-histone H3 antibody and analyzed *mkp-1* expression in the precipitated underlying DNA sequences. We found that costimulation with LPS and AEA, but not with LPS or AEA alone, resulted in enhanced histone H3 phosphorylation of the *mkp-1* gene sequence (Figure 7E). Thus, the rapid MKP-1 protein expression after LPS/AEA costimulation might be explained by histone modification and provides for the first time a link between cannabinoid-mediated signal transduction and regulation of "histone code" (Jenuwein and Allis, 2001).

Finally, we investigated whether $CB_{1/2}$ receptors or MKP-1 expression in BV-2 microglial cells (Figure 8A)

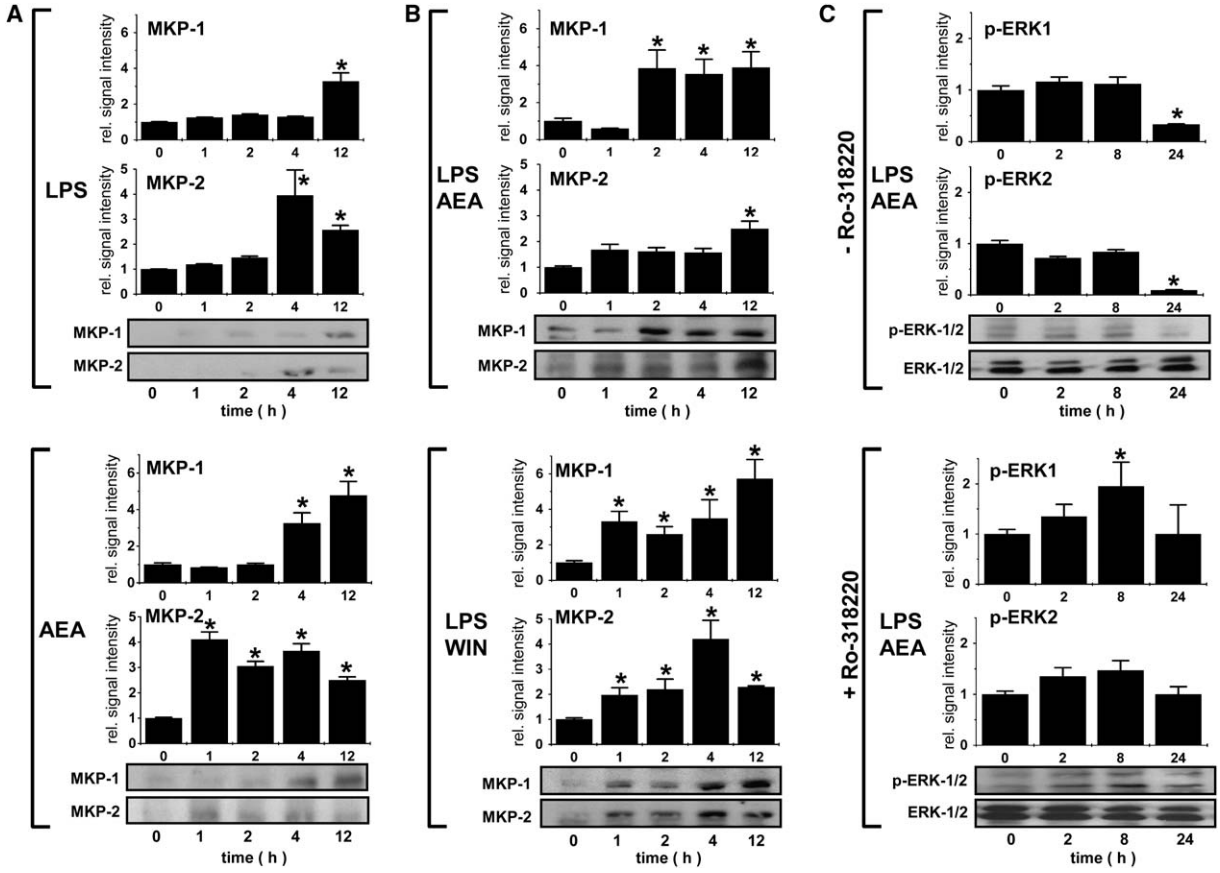

Figure 5. Expression of MKP-1 in Inflammatory Microglial Cells

(A) Induction of MKP-1 and MKP-2 expression in microglial cells in the presence of LPS or AEA. MKP-1 and MKP-2 expression is induced after incubation with AEA or LPS. BV-2 microglial cells were incubated with 10 μg/ml LPS (top) or with 2 μM AEA (bottom). Data are given as signal intensity of MKP-1 and MKP-2 relative to 0 min (mean ± S.D., n = 3). Asterisk, $p < 0.05$ (time points versus 0 min). One representative immunoblot is demonstrated.

(B) Induction of MKP-1 and MKP-2 expression in LPS-activated microglial cells in the presence of AEA or WIN-55,212,-2. MKP-1 and MKP-2 expression is induced rapidly in LPS-activated BV-2 microglial cells after incubation with 2 μM AEA (top) or 2 μM WIN 55,212-2, a $CB_{1/2}$-receptor agonist (bottom). Data are given as signal intensity of MKP-1 and MKP-2 relative to 0 min (mean ± S.D., n = 3). Asterisk, $p < 0.05$ (time points versus 0 min). One representative immunoblot is demonstrated.

(C) MKP expression inhibition abrogates dephosphorylation of ERK-1/2 by AEA in LPS-stimulated BV-2 microglia. BV-2 microglial cells were activated by 10 μg/ml LPS and 2 μM AEA with or without 10 μM Ro-318220, a MKP–expression inhibitor. Data are given as signal intensity of p-ERK-1 and p-ERK-2 relative to 0 min (mean ± S.D., n = 3). Asterisk, $p < 0.05$ (time points versus 0 min). One representative immunoblot is demonstrated.

and primary microglial cells (Figure 8B) were functionally involved in AEA-mediated neuroprotection in living brain tissue. As demonstrated in Figures 8A and 8B, CB_1 inhibition attenuated and CB2 inhibition abrogated neuroprotection by AEA in inflamed brain tissue. Moreover, inhibitor experiments with Ro-318220 as well as siRNA-silencing experiments confirmed that MKP-1 expression is also required for AEA-induced neuroprotection by BV-2 microglial cells (Figure 8A) as well as primary microglial cells (Figure 8B). In conclusion, AEA induced neuroprotection by $CB_{1/2}$-receptor stimulation and induction of MKP-1 expression in microglial cells of inflammatory brain lesions.

Discussion

Beside neurons, cells of the innate immune system are also capable of producing endocannabinoids (Walter and Stella, 2004), such as macrophages (Liu et al., 2003; Kuwae et al., 1999; Di Marzo et al., 1999) and microglial cells (Witting et al., 2004b), after stimulation. For instance, the binding of ATP to purinergic P2X7 receptors rapidly induces a Ca^{2+}-dependent release of endocannabinoids (Witting et al., 2004b), resulting in elevated concentrations in brain and spinal cord (Piomelli, 2003). Thus, endocannabinoids might represent a common messenger used by both the nervous and immune systems. In the mammalian brain, the CB_1 receptor is present in the neocortex, hippocampus, basal ganglia, cerebellum, and brainstem, where it is primarily found on glutamatergic and axon terminals of GABA interneurons and accounts for most of the behavioral actions of cannabinoid drugs (Chaperon and Thiebot, 1999; Herkenham et al., 1990). Because of its property as a $G_{i/o}$-coupled receptor, CB_1 can initiate signaling events typical of this class of transducing proteins, such as closure of Ca^{2+} channels, opening of K^+ channels, and inhibition of adenylyl cyclase activity, resulting in a decrease in

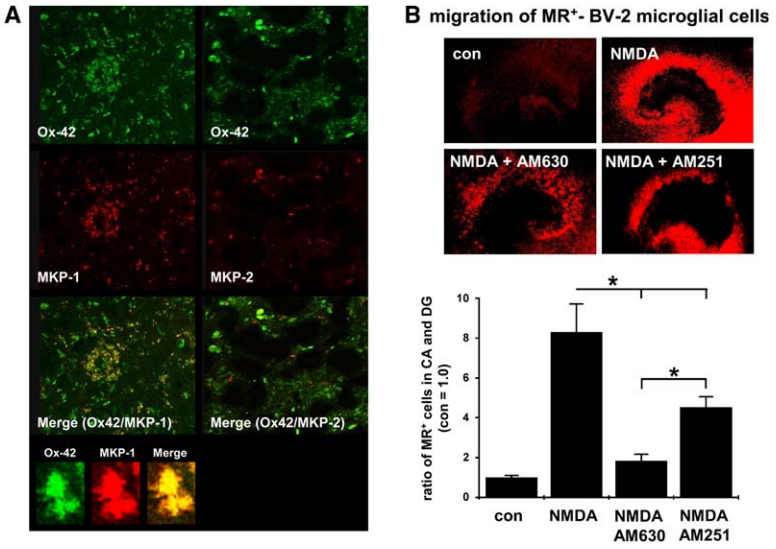

Figure 6. MKP Expression and CB1/2-Receptor Function in Tissue-Invading Microglial Cells

(A) Colocalization of MKP-1, but not MKP-2, with invading micoglial cells in inflammatory lesions of patients with multiple sclerosis. The colocalization of Ox42-positive microglial cells (green) and MKP-1-oder MKP-2-expressing cells (red) in inflammatory lesions of patients with MS is demonstrated (yellow in merger). The insert shows a representative picture of an MKP-1-expressing microglial cell in the inflammatory lesion.

(B) Migration of BV-2-microglial cells into the neuronal layers of living brain tissue. Site-specific migration of BV-2 microglial cells into the neuronal cell layers of NMDA damaged living organotypic brain slice cultures (OHSC). Results are given as fluorescence of Mini-Ruby-labeled (MR^+) BV-2 microglial cells in the neuronal layers after treatment relative to nondamaged brain tissue. Con, no treatment; AEA, incubation with 2 μM AEA; NMDA, induction of primary neuronal damage with 5 μM NMDA for 4 hr; AM251, 0.5 μM of the CB_1 receptor antagonist AM 251; AM 630, 2 μM of the CB_2 receptor antagonist AM 630. Data are given as mean ± S.D. (n = 6); asterisk = $p < 0.05$ (NMDA versus NMDA + AM251 or NMDA + AM630, NMDA + AM251 versus NMDA + AM630).

cytosolic cAMP (Howlett, 1984). Subsequently, regulation of neuronal gene expression by CB_1 depends on the recruitment of complex networks of intracellular protein kinases such as extracellular signal-regulated kinase (ERK) and focal adhesion kinase (FAK), which become activated when hippocampal brain tissue is treated with cannabinoid agonists (Derkinderen et al., 1996, 2003). In this context, cannabinoid receptors are

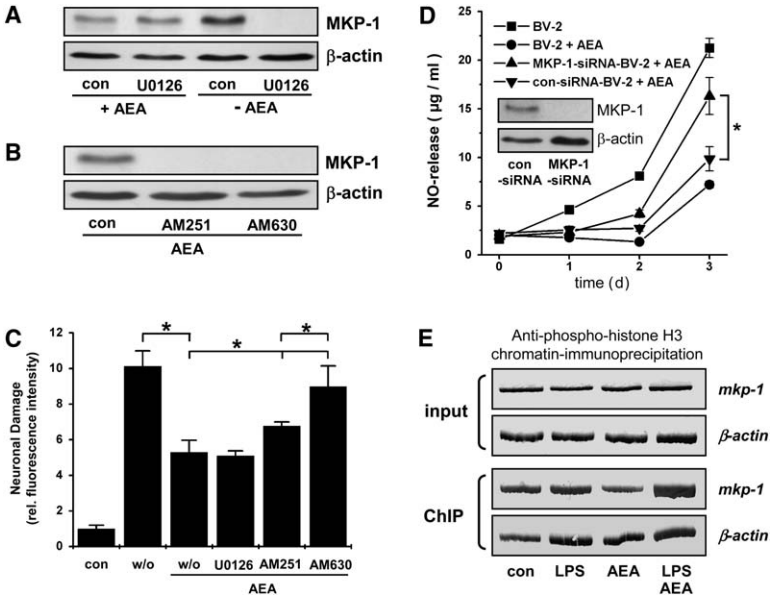

Figure 7. MKP-1 Expression and Neuroprotection after AEA Treatment Depends on $CB_{1/2}$ Activity, but Not on MAPK Activation, Is Associated by Rapid Phosphorylation of Histone H3 on the *mkp-1* Gene, and Suppresses Nitric Oxide Release in Living Brain Tissue

(A) AEA-induced MKP-1-expression is independent from MAPK activation. BV-2 microglial cells were stimulated for 12 hr with 10 μg/ml LPS with (+AEA) or without (−AEA) 2 μM AEA in the presence of 10 μM U0126, an inhibitor of MEK1/2. One representative immunoblot is demonstrated.

(B) AEA-induced MKP-1 expression depends on CB1- and CB2-receptor stimulation. BV-2 microglial cells were stimulated for 12 hr with 10 μg/ml LPS and 2 μM AEA in the presence of 0.5 μM AM 251 or 2 μM AM 630 or on the absence of CB1/2-receptor antagonists (con). One representative immunoblot is demonstrated.

(C) Propidium iodide fluorescence in the neuronal cell layers in NMDA-damaged OHSCs. Results are given as propidium iodide fluorescence in the neuronal layers after treatment relative to nondamaged brain tissue (con). Primary neuronal damage was induced with 5 μM NMDA for 4 hr before transfer of 10^5 BV-2 microglial cells (all other groups). AEA, 2 μM AEA; U0126, 10 μM of the MEK1/2-inhibitor U0126; AM251, 0.5 μM of the CB_1 receptor antagonist AM 251; AM 630, 2 μM of the CB_2 receptor antagonist AM 630; w/o, without inhibitors. Data are given as mean ± S.D. (n = 3); asterisk, $p < 0.05$ (AEA versus AEA + AM 630 and AEA + AM 251, AEA + AM 251 versus AEA + AM 630, AEA versus w/o).

(D) Reduction of NO release by AEA is MKP-1 dependent. Control-siRNA-transfected or MKP-1-siRNA-transfected BV-2 microglial cells were incubated with or without anandamide (AEA) before LPS stimulation. Data are given as mean ± S.D. (n = 3). Asterisk, $p < 0.05$ (MKP-1-siRNA-BV2 versus con-si-RNA-BV-2). The insert demonstrates downregulation of MKP-1 expression in AEA-treated BV-2 microglial cells by MKP-1 siRNA, which was 92.4% ± 5.6% compared to con siRNA.

(E) Enhanced association of phospho-histone H3 with mkp-1 gene sequence in LPS/AEA-treated BV-2 microglia cells. PCR of mkp-1 coding sequence is demonstrated in chromatin immunoprecipitation (ChIP) with monoclonal anti-phospho-histone H3-antibody or in input controls before chromatin immunoprecipitation. The precipitation controls (without antibody) were blank (not shown).

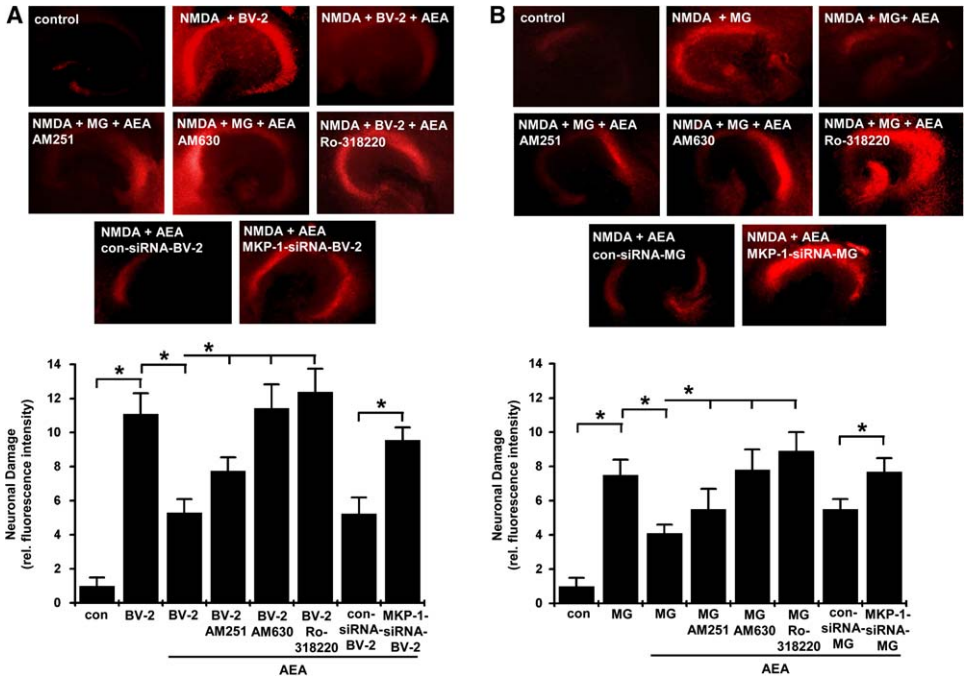

Figure 8. Neuroprotection by AEA Depends on $CB_{1/2}$ Receptors and Microglial MKP-1 Expression

(A) Propidium iodide fluorescence microscopy of the regions of neuronal injury in the cornu ammonis and dentate gyrus in living organotypic brain slice cultures after NMDA damage and invasion of BV-2 microglial cells. One representative picture is demonstrated in the top panel. Control, no treatment; AEA, incubation with 2 μM AEA; NMDA, induction of primary neuronal damage with 5 μM NMDA for 4 hr, BV-2, 3 days after transfer of 10^5 BV-2 microglial cells; AEA, 2 μM AEA; AM251, 0.5 μM of the CB_1 receptor antagonist AM 251; AM 630, 2 μM of the CB_2 receptor antagonist AM 630; Ro-318220, 10 μM Ro-318220; MKP-1-siRNA-BV-2, 3 days after transfer of 10^5 BV-2 microglial cells transfected with MKP-1-siRNA; con-siRNA-BV-2, 3 days after transfer of 10^5 BV-2 microglial cells transfected with control-siRNA. Bottom: results are given as propidium iodide fluorescence in the neuronal layers after treatment relative to nondamaged brain tissue. Data are given as mean ± S.D. (n = 3); asterisk, $p < 0.05$ (BV-2 + AM251, BV-2 + AM630, BV-2 + Ro-318220 versus BV-2, BV-2 versus BV-2 + AEA, con versus BV-2, MKP-1-siRNA-BV-2 versus con-siRNA-BV-2).

(B) Pictures of propidium iodide fluorescence microscopy of the regions of neuronal injury in the cornu ammonis and dentate gyrus in living organotypic brain slice cultures after NMDA damage and invasion of primary microglial cells. One representative picture is demonstrated in the top panel. Control, no treatment; AEA, incubation with 2 μM AEA; NMDA, induction of primary neuronal damage with 5 μM NMDA for 4 hr; MG, 3 days after transfer of 10^5 primary microglial cells; AEA, 2 μM AEA; AM251, 0.5 μM of the CB_1 receptor antagonist AM 251; AM 630, 2 μM of the CB_2 receptor antagonist AM 630; Ro-318220, 10 μM Ro-318220; MKP-1-siRNA-MG, 3 days after transfer of 10^5 primary microglial cells transfected with MKP-1-siRNA; con-siRNA-MG, 3 days after transfer of 10^5 primary microglial cells transfected with control-siRNA. Bottom: results are given as propidium iodide fluorescence in the neuronal layers after treatment relative to nondamaged brain tissue. Data are given as mean ± S.D. (n = 3); asterisk, $p < 0.05$ (MG + AM251, MG + AM630, MG + Ro-318220 versus MG, MG versus MG + AEA, con versus MG, MKP-1-siRNA-MG versus con-siRNA-MG).

coupled to the activation of ERK (Wartmann et al., 1995; Bouaboula et al., 1995a, 1995b, 1996) of c-*jun* N-terminal kinase and p38 mitogen-activated protein kinase (Liu et al., 2000; Rueda et al., 2000). Moreover, the CB_1 receptor is also coupled to the activation of protein kinase B (PKB) (Gomez del Pulgar et al., 2000). Taken together, in neuronal cells, cannabinoids inhibit the release of glutamate and other neurotransmitters by blunting membrane depolarisation and exocytosis (Schlicker and Kathmann, 2001).

Most of the effects of cannabinoids are mediated by their specific receptors, CB_1 and CB_2, which are coupled to adenyl cyclase (AC) through heterotrimeric $G_{i/o}$ proteins (Galve-Roperh et al., 2000; Guzman et al., 2001). However, in contrast to the CB_1 receptor, transduction systems responsible for CB_2 receptor signaling are less elucidated. CB_2 receptors are expressed mainly by cells of the immune system such as T cells, B cells, NK cells, monocytes, microglial cells, and neutrophil granulocytes (Galiegue et al., 1995). In these cells, inhibition of cAMP/protein kinase A (PKA) pathway may be responsible for the immunosuppressive action of cannabinoids by decreasing the expression of cAMP-responsive genes (Jacobsson et al., 2000). Moreover, CB_2 receptor might control immune-cell proliferation by coupling to ERK activation, independent of cAMP (Sarker et al., 2000). In our study, we demonstrated that cannabinoid-receptor stimulation is coupled to ERK activation via regulation of MKP-1 expression by histone H3 phosphorylation. In cells of the immune system, CB_2-receptor stimulation results in inhibitory signals (Walter and Stella, 2004), mediated by inhibition of cAMP/PKA pathway and inhibition of the transcription factors NF-AT und AP-1. We found that inhibitory signal transduction in microglial cells depends on parallel stimulation of pattern recognition receptors CD14/TLR4 by LPS. Endocannabinoids inhibit CB_2-mediated release of TNF-α, IL-1β, IL-6, and IL-8 by monocytes/macrophages (Klegeris et al., 2003; Berdyshev et al., 1997; Gallily et al., 2002), which we could confirm at least for IL-6 in microglial cells. Our findings

support the idea that endocannabinoids attracts microglial cells to the site of tissue damage by chemotaxis (Franklin et al., 2003; Franklin and Stella, 2003; Walter et al., 2003), where they help to control and limit local immune response in order to prevent harmful overactivation.

Here, we have found that the endocannabinoid AEA induced histone H3 phosphorylation, MKP-1 expression, and subsequent ERK-1/2 dephosphorylation in activated, but not in resting microglial cells, which in turn abolishes NO release and finally results in neuroprotection. Our data indicative for increased anandamide levels in MS lesions and previous studies reporting that synthetic $CB_{1/2}$-receptor agonists were capable of improving neurological outcome in a murine model of encephalomyelitis (Arevalo-Martin et al., 2003) are in line with our experimental findings about the protective role of endocannabinoid signaling in neuroinflammation. The clinical use of cannabinoids or cannabinoid receptor drugs for neuroprotective interventions during CNS inflammation (Jackson et al., 2005; Klein, 2005) and for treatment of MS are currently under discussion (Pryce and Baker, 2005; Thompson and Baker, 2002; Killestein et al., 2002). In our study, we conclude that release of the endocannabinoid AEA in injured brain tissue might act as a gatekeeper for signal transduction through the MAPK pathway and represent an important negative feedback loop within the CNS immune system needed to reduce the extent of the inflammatory response and to limit neurodegenerative immune reactions after primary brain damage. Moreover, endocannabinoid signaling strongly suppresses attack of microglial cells on nondamaged neurons, suggesting also a physiological function of the endocannabinoid system in maintaining a protective and healthy CNS microenviroment.

In conclusion, the endocannabinoid system represents a local messenger system between the nervous and immune system and is obviously involved in the control of immune activation and neuroprotection. Therefore, elucidating the pathology of the endocannabinoid system during neuroinflammation and neurodegeneration might open new avenues of therapeutic interventions in the future.

Experimental Procedures

Cell Cultures

BV-2 murine microglial cells, which exhibit morphologic and functional properties comparable to primary microglial cells (Ullrich et al., 2001; Bocchini et al., 1992), were cultured in DMEM medium supplemented with 10% FCS at a density not exceeding 2×10^5 cells/ml. Microglial activation was performed by incubation with 10 μg/ml LPS (Sigma, St. Louis, MO) in the presence or absence of 2 μM, 5 μM, or 10 μM anandamide (Sigma) or 2 μM, 5 μM, or 10 μM WIN 55,212-2 (Sigma). Labeling of microglial cells was performed by incubation with culture medium containing 20 μg/ml Mini-Ruby (MR), a 10 kDa dextran amine, conjugated with rhodamine (Molecular Probes, Eugene, OR). Primary microglia cells were prepared from newborn mice with a modification (Ullrich et al., 2001) of the technique described by Giulian and Baker (Giulian and Baker, 1986). The obtained primary microglia cell cultures were >95% pure. In vitro experiments revealed no toxic effects of the inhibitors and substances used (AEA, Ro-218200, U0126, AM221, AM630) on cultures of BV-2 microglial cells or primary microglial cells up to 3 days in the concentrations used in this study.

Primary neuronal cultures of cerebral cortex were obtained from embryos (E16-E18) of Wistar rats (Bundesinstitut für gesundheitlichen Verbraucherschutz und Veterinärmedizin, Berlin, Germany). Cultures were prepared according to Brewer (1995). Excitotoxic damage was induced by 5 μM NMDA for 4 hr. For oxygen glucose deprivation (OGD), medium was removed from the cultures and preserved, and cells were rinsed twice with PBS and then subjected to OGD for 60 min in a balanced salt solution at $pO_2 < 2$ mm Hg, followed by replacement of the preserved medium as described previously (Bruer et al., 1997). Neuronal injury was quantitatively assessed by measurement of LDH activity in the medium after NMDA or OGD exposure.

Investigations of Human Brain Tissue

Fresh frozen blocks of autopsied brain tissue from patients with chronic active MS (n = 5), chronic silent MS (n = 6), and control patients (n = 7) were provided by two of us (C.S.R. and C.M.) on dry ice (mean age/postmortem delay: 38 years/6.4 ± 2.1 hr for patients with chronic active MS, 49 years/3.5 ± 0.9 hr for patients with chronic silent MS and 56 years/7.6 ± 1.3 hr for control patients). CNS tissue from chronic active cases contained established, gliotic lesions with evidence of recent inflammatory activity at the lesion margins, and some fresh, acute MS lesions with edema, actively demyelinating margins rich in inflammatory cells and numerous hypertrophic astrocytes. Chronic silent cases displayed lesions that were intensely gliotic and demyelinated with little evidence of inflammation. The 16 brain samples were assigned numbers and studied by investigators blinded to the code.

Analysis of endocannabinoids were performed by GC/MS (Witting et al., 2004a). 10 μm thick sections were briefly air dried and then immersed in ice-cold acetone for 10 min. After incubation with blocking buffer, sections were incubated with primary antibodies against Ox42 (Abcam, Cambrigdeshire, UK, 1:200 dilution) and MKP-1 or MKP-2 primary antibodies (Santa Cruz, CA, 1:200 dilution) for 1 hr at room temperature. Slides were then incubated with secondary antibodies conjugated to Cy2 (Jackson Laboratories, 1:50, for Ox42 detection) or RedX (Jackson Laboratories, 1:50, for MKP-1 or MKP-2 detection). The sections were mounted in DPX (Fluka, Neu-Ulm, Germany) and examined with a Leica TCS-NT laser scanning confocal microscope (Heidelberg, Germany).

Preparation of Organotypic Hippocampal Slice Cultures and Analysis of Inflammatory Neuronal Cell Death

OHSCs were obtained by decapitating newborn mice on the ninth to tenth postnatal day, aseptically removing a frontal slice of the caudal cerebrum and transversally sectioning it at a 350 μm thickness on a sliding vibratome in MEM supplemented with 1% L-glutamine as described earlier (Bocchini et al., 1992). OHSCs were cultured in culture medium (MEM:HBSS 2:1, 25% normal horse serum, 2% L-glutamine, 2.64 mg/ml glucose and penicillin/streptomycin) at 35ºC and 5% CO_2 for 10 days in vitro to ensure a healthy organotypic microenvironment in the middle layer of the OHSCs, which is known to induce microglial ramification (Ullrich et al., 2001; Diestel et al., 2003; Bocchini et al., 1992). OHSCs were exposed to 5 μM NMDA for 4 hr, after which the medium was exchanged.

BV-2 microglial cells (10^5 cells/OHSC) were transferred onto the surface of OHSCs that had been cultured for 10 days. With this approach, the proportion of endogenous primary microglial cells is less than 5% of the total microglial cell count (Ullrich et al., 2001). 3 days after transferring the microglial cells, cell death at the sites of neuronal injury (neuronal cell layers of cornu ammonis, CA, and dentate gyrus, DG) was detected according to Adamchik et al. (Adamchik et al., 2000) by the addition of 5 μg/ml propidium iodide (PI) to fresh medium and incubation for 15 min. Dead cells within the neuronal cell layers was quantified by fluorescence microscopy with a BX-50 microscope (Olympus, Tokyo, Japan). Propidium-iodide fluorescence was selectively quantified in stratum granulare of the dentate gyrus and stratum pyramidale of the cornu ammonis (identified by bright field microscopy) by computer-assisted quantitative approach. Within these layers, almost exclusively neurons are located (granule cells in the dentate and pyramidal cells in the cornu ammonis). Fluorescence intensities obtained in the neuronal cell layers only were corrected by the overall fluorescence measured throughout the slice. Additional cell counts gave the same quantitative results. Correlation between fluorescence intensity and total numbers of dead cells inside the hippocampal neuronal layers was linear

between 1×10^4 and 2×10^5 cells and not linear (saturation) above 2×10^5 cells. The low limit of quantification was 4×10^3 cells; differences of 5×10^3 dead cells resulted in significant changes in fluorescence intensity. Numbers of dead neuronal cells within the non-treated control slice tissues were between 1×10^4 and 2×10^4 cells.

CB_1 receptors were inhibited by 0.5 μM of AM 251 (N-[Piperidin-1-yl]-5-[4-iodophenyl]-1-[2,4-dichlorophenyl]-4-methyl-1H-pyrazole-3-carboxamide, Tocris), CB_2 receptors were inhibited by 2 μM AM 630 (6-Iodo-2-methyl-1-[2-(4-morpholinyl)ethyl]-1H-indol-3-yl](4-methoxyphenyl)methanone, Tocris), MKP-1-expression was inhibited by 10 μM Ro-318220 (2-{1-[3-(Amidinothio)propyl]-1H-indol-3-yl}-3-(1-methylindol-3-yl)maleimide Methanesulfonate, Sigma Aldrich, Deisenhofen, Germany), and MAPK-activation by 10 μM U0126 (1,4-diamino-2,3-dicyano-1,4-bis[2-aminophenylthio] butadiene, Cell Signaling, Beverly, MA).

Cell-Culture Experiments

Cells were lysed by repeated freeze-thawing cycles, and lysates were used for experiments. Proteins were separated by 12% SDS/PAGE, transblotted onto nitrocellulose membranes. The membranes were incubated with antibodies directed against phospo-ERK-1/2, ERK-1/2, phosphor-MEK, MEK (Cell Signaling, Beverly, MA) and iNOS (Sigma, St. Louis, MO). After incubation with an appropriate peroxidase-conjugated secondary antibody, the blots were developed with a chemoluminescence (ECL) detection kit (Amersham, Buckinghamshire, UK). Densitometric analysis was performed by MetaMorph software, version 3.6a (Universal Imaging Corp, West Chester, PA), relative to the 0 min signal and background normalization. Statistical analysis was performed by the Wilcoxon test ($p < 0.05$). Cannabinoid receptor antibodies for functional blocking were obtained from Biomol (Hamburg, Germany). The release of nitric oxide was determined in a nitroblue tetrazolium assay and the release of IL-6 and TNF-α by ELISA (Pharmingen, San Diego, CA). SiRNA transfection against MKP-1 was performed according to the protocol of Santa Cruz (Santa Cruz, CA) with transfection medium, transfection reagent, MKP-1-siRNA (sc-35938), and control siRNA (sc-35938) from Santa Cruz. Reduction of MKP-1 protein levels after siRNA transfection have been quantified densitometrically in Western blot anaysis and was 89.5% ± 8.2%. Chromatin immunoprecipitation was performed with a kit from Upstate (Waltham, MA) according to the manufacturer's recommendation with a mouse monoclonal phospho-histone H3 antibody (Sigma, St. Louis, MO). PCR analyses were performed with the following primer pairs: 5′-TCAGCGGGGAGTTTTTGTG-3′ and 5′-CTGTGAGTGACCCTCAAAG TGG-3′ for mkp-1 and 5′-AACACCCCAGCCATGTACG-3′ and 5′-AT GTCACGCACGATTTCCC-3′ for β-actin according to Li et al. (Li et al., 2001).

Acknowledgments

We thank Ms. Anja Graefe and Ms. Doreen Luedecke for their excellent technical assistance and Ms. Kimberley Rosegger for her excellent secretarial assistance. This study was supported by the Research Network N2 of the State Saxony-Anhalt of Germany (O.U.) and a grant from the Deutsche Forschungsgemeinschaft to R.N., O.U., and R.S.S. and National Institutes of Health grants (NS 08952 and NS 11920) to C.S.R. We thank the University of Miami Human Brain Bank (Dr. C. Petito—N01-H0-8-3284) and the Manhattan Brain Bank (Dr. S. Morgello—R24MH59724) for normal human brain samples.

Received: May 20, 2005
Revised: September 17, 2005
Accepted: November 2, 2005
Published: January 4, 2006

References

Adamchik, Y., Frantseva, M.V., Weisspapir, M., Carlen, P.L., and Perez Velazquez, J.L. (2000). Methods to induce primary and secondary traumatic damage in organotypic hippocampal slice cultures. Brain Res. Brain Res. Protoc. *5*, 153–158.

Alger, B.E. (2002). Retrograde signaling in the regulation of synaptic transmission: focus on endocannabinoids. Prog. Neurobiol. *68*, 247–286.

Arevalo-Martin, A., Vela, J.M., Molina-Holgado, E., Borrell, J., and Guaza, C. (2003). Therapeutic action of cannabinoids in a murine model of multiple sclerosis. J. Neurosci. *23*, 2511–2516.

Berdyshev, E.V., Boichot, E., Germain, N., Allain, N., Anger, J.P., and Lagente, V. (1997). Influence of fatty acid ethanolamides and delta-9-tetrahydrocannabinol on cytokine and arachidonate release by mononuclear cells. Eur. J. Pharmacol. *330*, 231–240.

Bocchini, V., Mazzolla, R., Barluzzi, R., Blasi, E., Sick, P., and Kettenmann, H. (1992). An immortalized cell line expresses properties of activated microglial cells. J. Neurosci. Res. *31*, 616–621.

Bouaboula, M., Bourrie, B., Rinaldi-Carmona, M., Shire, D., Le Fur, G., and Casellas, P. (1995a). Stimulation of cannabinoid receptor CB1 induces krox-24 expression in human astrocytoma cells. J. Biol. Chem. *270*, 13973–13980.

Bouaboula, M., Poinot Chazel, C., Marchand, J., Canat, X., Bourrie, B., Rinaldi Carmona, M., Calandra, B., Le Fur, G., and Casellas, P. (1995b). Activation of mitogen-activated protein kinases by stimulation of the central cannabinoid receptor CB1. Biochem. J. *312*, 637–641.

Bouaboula, M., Poinot Chazel, C., Marchand, J., Canat, X., Bourrie, B., Rinaldi Carmona, M., Calandra, B., Le Fur, G., and Casellas, P. (1996). Signaling pathway associated with stimulation of CB2 peripheral cannabinoid receptor. Involvement of both mitogen-activated protein kinase and induction of Krox-24 expression. Eur. J. Biochem. *237*, 704–711.

Brewer, G.J. (1995). Serum-free B27/neurobasal medium supports differentiated growth of neurons from the striatum, substantia nigra, septum, cerebral cortex, cerebellum and dentate gyrus. J. Neurosci. Res. *42*, 674–683.

Bruer, U., Weih, M.K., Isaev, N.K., Meisel, A., Ruscher, K., Bergk, A., Trendelenburg, G., Wiegand, F., Victorov, I.V., and Dirnagl, U. (1997). Induction of tolerance in rat cortical neurons: hypoxic preconditioning. FEBS Lett. *414*, 117–121.

Carrier, E.J., Kearn, C.S., Barkmeier, A.J., Breese, N.M., Yang, W., Nithipatikom, K., Pfister, S.L., Campbell, W.B., and Hillard, C.J. (2004). Cultured rat microglial cells synthesize the endocannabinoid 2-arachidonylglycerol, which increases proliferation via a CB2 receptor dependent mechanism. Mol. Pharmacol. *65*, 999–1007.

Chaperon, F., and Thiebot, M.H. (1999). Behavioral effects of cannabinoid agents in animals. Crit. Rev. Neurobiol. *13*, 243–281.

Derkinderen, P., Toutant, M., Burgaya, F., Le Bert, M., Siciliano, J.C., de Franciscis, V., Gelman, M., and Girault, J.A. (1996). Regulation of a neuronal form of focal adhesion kinase by anandamide. Science *273*, 1719–1722.

Derkinderen, P., Valjent, E., Toutant, M., Corvol, J.C., Enslen, H., Ledent, C., Trzaskos, J., Caboche, J., and Girault, J.A. (2003). Regulation of extracellular signal-regulated kinase by cannabinoids in hippocampus. J. Neurosci. *23*, 2371–2382.

Diestel, A., Aktas, O., Hackel, D., Häke, I., Meier, S., Raine, C.S., Nitsch, R., Zipp, F., and Ullrich, O. (2003). Activation of microglial poly(ADP-ribose)-polymerase-1 by cholesterol breakdown products during neuroinflammation: a link between demyelination and neuronal damage. J. Exp. Med. *198*, 1729–1740.

Di Marzo, V., Fontana, A., Cadas, H., Schinelli, S., Cimino, G., Schwartz, J.C., and Pomelli, D. (1994). Formation and inactivation of endogenous cannabinoid anandamide in central neurons. Nature *372*, 686–691.

Di Marzo, V., Bisogno, T., de Petrocellis, L., Melck, D., Orlando, P., Wagner, J.A., and Kunos, G. (1999). Biosynthesis and inactivation of the endocannabinoid 2-arachidonoylglycerol in circulating and tumoral macrophages. Eur. J. Biochem. *264*, 258–267.

Facchinetti, F., Del Giudice, E., Furegato, S., Passarotto, M., and Leon, A. (2003). Cannabinoids ablate release of TNFα in rat microglial cells stimulated with lypopolysaccharide. Glia *41*, 161–168.

Franklin, A., and Stella, N. (2003). Arachidonylcyclopropylamide increases microglial cell migration through cannabinoid CB2 and

abnormal-cannabidiol-sensitive receptors. Eur. J. Pharmacol. *474*, 195–198.

Franklin, A., Parmentier-Batteur, S., Walter, L., Greenberg, D.A., and Stella, N. (2003). Palmitoylethanolamide increases after focal cerebral ischemia and potentiates microglial cell motility. J. Neurosci. *23*, 7767–7775.

Galiegue, S., Mary, S., Marchand, J., Dussossoy, D., Carriere, D., Carayon, P., Bouaboula, M., Shire, D., Le Fur, G., and Casellas, P. (1995). Expression of central and peripheral cannabinoid receptors in human immune tissue and leukocyte subpopulations. Eur. J. Biochem. *232*, 54–61.

Gallily, R., Breuer, A., and Mechoulam, R. (2002). 2-arachidonylglycerol, an endogenous cannabinoid, inhibits tumor necrosis factor-alpha production in murine macrophages, and in mice. Eur. J. Pharmacol. *406*, 5–7.

Galve-Roperh, I., Sanchez, C., Cortes, L., del Pulgar, T.G., Izquierdo, M., and Guzman, M. (2000). Anti-tumoral action of cannabinoids: involvement of sustained ceramide accumulation and extracellular signal regulated kinase activation. Nat. Med. *6*, 313–319.

Giuffrida, A., Parsone, L.H., Kerr, T.M., Rodriguez de Fonseca, F., Navarro, M., and Pomelli, D. (1999). Dopamine activation of endogenous cannabinoid signaling in dorsal striatum. Nat. Neurosci. *2*, 358–363.

Giulian, D., and Baker, T.J. (1986). Characterization of ameboid microglia isolated from developing mammalian brain. J. Neurosci. *6*, 2163–2178.

Gomez del Pulgar, T., Velasco, G., and Guzman, M. (2000). The CB1 cannabinoid receptor is couplet to the activation of protein kinase B/Akt. Biochem. J. *347*, 369–373.

Guo, Y.L., Kang, B., and Williamson, J.R. (1998). Inhibition of the expression of mitogen activated protein phosphatase-1 potentiates apoptosis induced by tumor necrosis factor-alpha in rat mesangial cells. J. Biol. Chem. *273*, 10362–10366.

Guzman, M., Sanchez, C., and Galve-Roperh, I. (2001). Control of the cell survival/death decision by cannabinoids. J. Mol. Med. *78*, 613–625.

Hansen, H.H., Schmid, P.C., Bittigau, P., Lastres-Becker, I., Berrendero, F., Manzanares, J., Ikonomidou, C., Schmid, H.H.O., Fernandez-Ruiz, J.J., and Hansen, H.S. (2001). Anandamide, but not 2-arachidonoylglycerol, accumulates during in vivo neurodegeneration. J. Neurochem. *78*, 1415–1427.

Hemmer, B., Archelos, J.J., and Hartung, H.P. (2002). New concepts in the immunopathogenesis of multiple sclerosis. Nat. Rev. Neurosci. *3*, 291–301.

Heppner, F.L., Skutella, T., Hailer, N.P., Haas, D., and Nitsch, R. (1998). Activated microglial cells migrate towards site of excitotoxic neuronal injury inside organotypic hippocampal slice cultures. Eur. J. Neurosci. *10*, 3284–3290.

Herkenham, M., Lynn, A.B., Little, M.D., Johnson, M.R., Melvin, L.S., de Costa, B.R., and Rice, K.C. (1990). Cannabinoid receptor localization in brain. Proc. Natl. Acad. Sci. USA *87*, 1932–1936.

Howlett, A.C. (1984). Inhibition of neuroblastoma adenylate cyclase by cannabinoid and nantradol compounds. Life Sci. *35*, 1803–1813.

Jacobsson, S.O., Rongard, E., Stridh, M., Tiger, G., and Fowler, C.J. (2000). Serum-dependent effects of tamoxifen and cannabinoids upon C6 glioma cell viability. Biochem. Pharmacol. *60*, 1807–1813.

Jackson, S.J., Diemel, L.T., Pryce, G., and Baker, D. (2005). Cannabinoids and neuroprotection in CNS inflammatory disease. J. Neurol. Sci. *233*, 21–25.

Jenuwein, T., and Allis, C.D. (2001). Translating the histone code. Science *293*, 1074–1080.

Killestein, J., Hoogervorst, E.L., Reif, M., Kalkers, N.F., Van Loenen, A.C., Staats, P.G., Gorter, R.W., Uitdehaag, B.M., and Polman, C.H. (2002). Safety, tolerability, and efficacy of orally administered cannabinoids in MS. Neurology *58*, 1404–1407.

Klegeris, A., Bissonnette, C.J., and McGeer, P.L. (2003). Reduction of human monocytic cell neurotoxicity and cytokine secretion by ligands of the cannabinoid-type CB2 receptor. Br. J. Pharmacol. *139*, 775–786.

Klein, T.W. (2005). Cannabinoid-based drugs as anti-inflammatory therapeutics. Nat. Rev. Immunol. *5*, 400–411.

Kreitzer, A.C., and Regehr, W.G. (2001). Retrograde inhibition of presynaptic calcium influx by endogenous cannabinoids at excitatory synapses onto Purkinje cells. Neuron *29*, 717–727.

Kuwae, T., Shiota, Y., Schmid, P.C., Krebsbach, R., and Schmid, H.H. (1999). Biosynthesis and turnover of anandamide and other N-acylethanolamines in peritoneal macrophages. FEBS Lett. *459*, 123–127.

Laake, J.H., Haug, F.M., Wieloch, T., and Ottersen, O.P. (1999). A simple in vitro model of ischemia based on hippocampal slice cultures and propidium iodide fluorescence. Brain Res. Brain Res. Protoc. *4*, 173–184.

Llano, I., Leresche, N., and Marty, A. (1991). Calcium entry increases the sensitivity of cerebellar Purkinje cells to applied GABA and decreases inhibitory synaptic currents. Neuron *6*, 565–574.

Li, J., Gorospe, M., Hutter, D., Barnes, J., Keyse, S.M., and Liu, Y. (2001). Transcriptional induction of MKP-1 in response to stress is associated with histone H3 phosphorylation acetylation. Mol. Cell. Biol. *21*, 8213–8224.

Liu, J., Gao, B., Mirshahi, F., Sanyal, A.J., Khanolkar, A.D., Makriyanis, A., and Kunos, G. (2000). Functional CB1 cannabinoid receptors in human vascular endothelial cells. Biochem. J. *346*, 835–840.

Liu, J., Batkai, S., Pacher, P., Harvey-White, J., Wagner, J.A., Cravatt, B.F., Gao, B., and Kunos, G. (2003). Lipopolysaccharide induces anandamide synthesis in macrophages via CD14/MAPK/phosphoinositide 3-kinase/NF-kappaB independently of platelet-activating factor. J. Biol. Chem. *278*, 45034–45039.

Mabuchi, T., Kitagawa, K., Ohtsuki, T., Kuwabara, K., Yagita, Y., Yanagihara, T., Hori, M., and Matsumoto, M. (2000). Contribution of microglia/macrophages to expansion of infarction and response of oligodendrocytes after focal cerebral ischemia in rats. Stroke *31*, 1735–1743.

Marsicano, G., Goodenough, S., Monory, K., Hermann, H., Eder, M., Cannich, A., Azad, S.C., Cascio, M.G., Gutiérrez, S.O., van der Stelt, M., et al. (2003). CB1 cannabinoid receptors and on-demand defense against excitotoxicity. Science *302*, 84–88.

Matsuda, L.A., Lolait, S.J., Brownstein, M.J., Young, A.C., and Bronner, T.I. (1988). Structure of a cannabinoid receptor in rat brain. Mol. Pharmacol. *34*, 605–613.

Mechoulam, R., and Lichtman, A.H. (2003). Stout guards of the central nervous system. Science *302*, 65–67.

Mechoulam, R., Ben-Shabat, S., Hanus, L., Ligumsky, M., Kaminski, N.E., Schatz, A.R., Gopher, A., Almog, S., Martin, B.R., Compton, D.R., et al. (1995). Identification of an endogenous 2-monoglyceride, present in canine gut, that binds to cannabinoid receptors. Biochem. Pharmacol. *50*, 83–90.

Munro, S., Thomas, K.L., and Abu-Shaar, M. (1993). Molecular characterization of a peripheral receptor for cannabinoids. Nature *365*, 61–65.

Panikashvili, D., Simeonidou, C., Ben-Shabat, S., Hanus, L., Breuer, A., Mechoulam, R., and Shohami, E. (2001). An endogenous cannabinoid (2-AG) is neuroprotective after brain injury. Nature *413*, 527–531.

Piomelli, D. (2003). The molecular logic of endocannabinoid signalling. Nat. Rev. Neurosci. *4*, 873–884.

Piomelli, D., and Greengard, P. (1990). Lipoxygenase metabolites of arachidonic acid in neuronal transmembrane signalling. Trends Pharmacol. Sci. *11*, 367–373.

Pryce, G., and Baker, D. (2005). Emerging properties of cannabinoid medicines in management of multiple sclerosis. Trends Neurosci. *28*, 272–276.

Rueda, D., Galve-Roperh, I., Haro, A., and Guzman, M. (2000). The CB1 cannabinoid receptor is coupled to the action of c-Jun N-terminal kinase. Mol. Pharmacol. *58*, 814–820.

Sarker, K.P., Obara, S., Nakata, M., Kitajima, I., and Maruyama, I. (2000). Anandamide induces apoptosis of PC-12 cells: involvement of superoxide and caspase-3. FEBS Lett. *472*, 34–44.

Schlicker, E., and Kathmann, M. (2001). Modulation of transmitter release via presynaptic cannabinoid receptors. Trends Pharmacol. Sci. *22*, 565–572.

Shapiro, P.S., and Ahn, N.G. (1998). Feedback regulation of Raf-1 and mitogen-activated protein kinase (MAP) kinase kinases 1 and 2 by MAP kinase phosphatase-1 (MKP-1). J. Biol. Chem. *273*, 1788–1793.

Stoll, G., Jander, S., and Schroeter, M. (1998). Inflammation and glial responses in ischemic brain lesions. Prog. Neurobiol. *56*, 149–171.

Sugiura, T., Kondo, S., Sukagawa, A., Nakane, S., Shinoda, A., Itoh, K., Yamashita, A., and Waku, K. (1995). 2-arachidonoylglycerol: a possible endogenous cannabinoid receptor ligand in brain. Biochem. Biophys. Res. Commun. *215*, 89–97.

Thompson, A.J., and Baker, D. (2002). Cannabinoids in MS: potentially useful but not just yet! Neurology *58*, 1323–1324.

Trapp, B.D., Peterson, J., Ransohoff, R.M., Rudick, R.A., Mork, S., and Bo, L. (1998). Axonaltransection in the lesions of multiple sclerosis. N. Engl. J. Med. *338*, 278–285.

Trettel, J., and Levine, E.S. (2003). Endocannabinoids mediate rapid retrograde signaling at interneuron right-arrow pyramidal neuron synapses of the neocortex. J. Neurophysiol. *89*, 2334–2338.

Ullrich, O., Diestel, A., Eyüpoglu, I.Y., and Nitsch, R. (2001). Regulation of microglial expression of integrins by poly(ADP-ribose)polymerase-1. Nat. Cell Biol. *3*, 1035–1042.

Waksman, Y., Olson, J.M., Carlisle, S.J., and Cabral, G.A. (1999). The central cannabinoid receptor (CB1) mediates inhibition of nitric oxide production by rat microglial cells. J. Pharmacol. Exp. Ther. *288*, 1357–1366.

Walker, J.M., Huang, S.M., Strangman, N.M., Tsou, K., and Sañudo-Peña, M.C. (1999). Pain modulation by release of the endogenous cannabinoid anandamide. Proc. Natl. Acad. Sci. USA *96*, 12198–12203.

Walter, L., and Stella, N. (2004). Cannabinoids and neuroinflammation. Br. J. Pharmacol. *141*, 775–785.

Walter, L., Franklin, A., Witting, A., Wade, C., Xie, Y., Kunos, G., Mackie, K., and Stella, N. (2003). Nonpsychotropic cannabinoid receptors regulate microglial cell migration. J. Neurosci. *23*, 1398–1405.

Wartmann, M., Campbell, D., Subramanian, A., Burstein, S.H., and Davis, R.J. (1995). The MAP kinase signal transduction pathway is activated by the endogenous cannabinoid anandamide. FEBS Lett. *359*, 133–136.

Wilson, R.I., and Nicoll, R.A. (2002). Endocannabinoid signaling in the brain. Science *296*, 678–682.

Witting, A., Weydt, P., Hong, S., Kliot, M., Moller, T., and Stella, N. (2004a). Endocannabinoids accumulate in spinal cord of SOD^{G93A} transgenic mice. J. Neurochem. *89*, 1555–1557.

Witting, A., Walter, L., Wacker, J., Moller, T., and Stella, N. (2004b). P2X7 receptors control 2-arachidonoylglycerol production by microglial cells. Proc. Natl. Acad. Sci. USA *101*, 3214–3219.